

Electronic polarization at surfaces and thin films of organic molecular crystals: PTCDA

E.V. Tsiper^(a), Z.G. Soos^(a), W. Gao^(b), and A. Kahn^(b)

^(a)Department of Chemistry, Princeton University, Princeton, NJ 08544

^(b)Department of Electrical Engineering, Princeton University, Princeton, NJ 08544

(May 2, 2002)

The electronic polarization energies, $P = P_+ + P_-$, of a PTCDA (perylene-tetracarboxylic acid dianhydride) cation and anion in a crystalline thin film on a metallic substrate are computed and compared with measurements of the PTCDA transport gap on gold and silver. Both experiments and theory show that P is 500 meV larger in a PTCDA monolayer than in 50 Å films. Electronic polarization in systems with surfaces and interfaces are obtained self-consistently in terms of charge redistribution within molecules.

I. TRANSPORT GAP

The electronic structure of organic molecular crystals is strikingly different from the conventional inorganic semiconductors, such as Si, in that the electronic polarization of the dielectric medium by charge carriers constitutes a major effect, with energy scale greater than transfer integrals or temperature [1,2]. The transport gap E_t for creating a separated electron-hole pair has a substantial (1–2 eV) polarization energy contribution [3] and exceeds the optical gap by ~ 1 eV. Limited overlap rationalizes the modest mobilities of organic molecular solids. Devices such as light-emitting diodes, thin film transistors, or photovoltaic cells require charge transport and are consequently based on thin films, quite often deposited on metallic substrates [4,5]. Organic electronics relies heavily on controlling films with monolayer precision, on forming structures with several thin films, and on characterizing the interfaces. The positions of transport states and mechanisms for charge injection are among the outstanding issues for exploiting organic devices. We focus here on the electronic polarization of crystalline thin films near surfaces and interfaces. We find that electronic polarization, and hence E_t , in a prototypical organic crystal is significantly different at a free surface, near a metal-organic interface, in thin organic layers, and in the bulk.

Weak intermolecular forces characterize organic molecular crystals, whose electronic and vibrational spectra are readily related to gas-phase transitions [1,2]. Due to small transfer integrals, charge carriers are molecular ions embedded in the lattice of neutral molecules. The transport gap E_t in the crystal is derived from the charge gap for electron transfer in the gas phase, $I(g) - A(g)$, which is the difference between the ionization potential and the electron affinity. But crystals have electrostatic interactions even in the limit of no overlap, and charge carriers are surrounded by self-consistent polarization clouds. In contrast to polaronic effects, electronic polarization is instantaneous and directly affects the positions of energy levels. Formation of polarization clouds is

associated with stabilization energy P_+ for cations (the “holes”) and P_- for anions (the “electrons”). The combination $P = P_+ + P_-$ occurs in $E_t = I(g) - A(g) - P$. Since Coulomb interactions are long-ranged, polarization clouds extend over many lattice constants and P depends on the proximity to surfaces and interfaces.

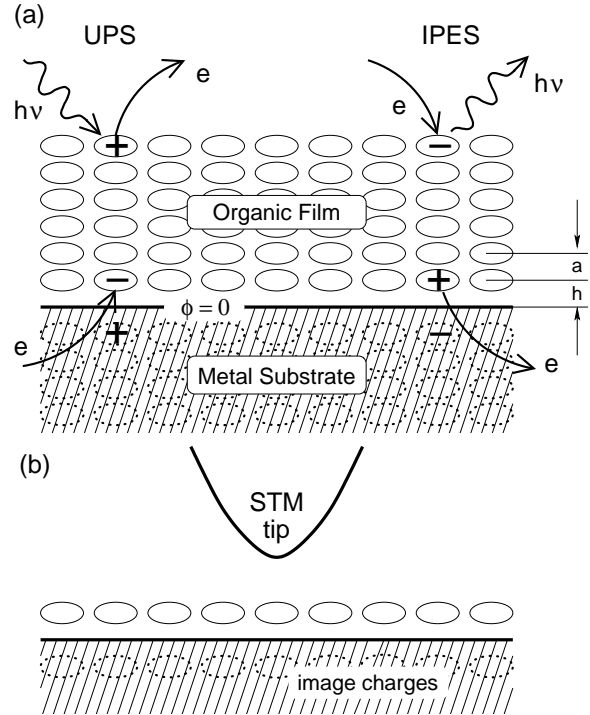


Fig. 1 Schematic representation of charge-generation processes in crystalline molecular films. (a) UPS/IPES generates a cation/anion at the outer surface, while charge injection from the substrate involves the layer next to the metal. (b) Tunneling through a monolayer. Dashed ovals in (a) and (b) represent image charges in the metal.

Figure 1(a) depicts schematically an ultraviolet photoemission (UPS) process where the ejected electron leaves behind a molecular cation in the outermost layer. In inverse photoelectron spectroscopy (IPES), the surface

is irradiated with low-energy electrons and the emitted photon is detected when an electron is captured to form a molecular anion. UPS data is increasingly available from sub-monolayer to $\sim 100\text{\AA}$ films [6], while the IPES data is more limited. The combination of UPS with IPES yields E_t directly, with P about 1–2 eV in representative organic materials used in devices [3]. As sketched in Fig. 1(b), tunneling electron spectroscopy gives E_t as the interval between the differential conductance peaks when the potential of the tip matches either the electron or the hole transport levels of the film.

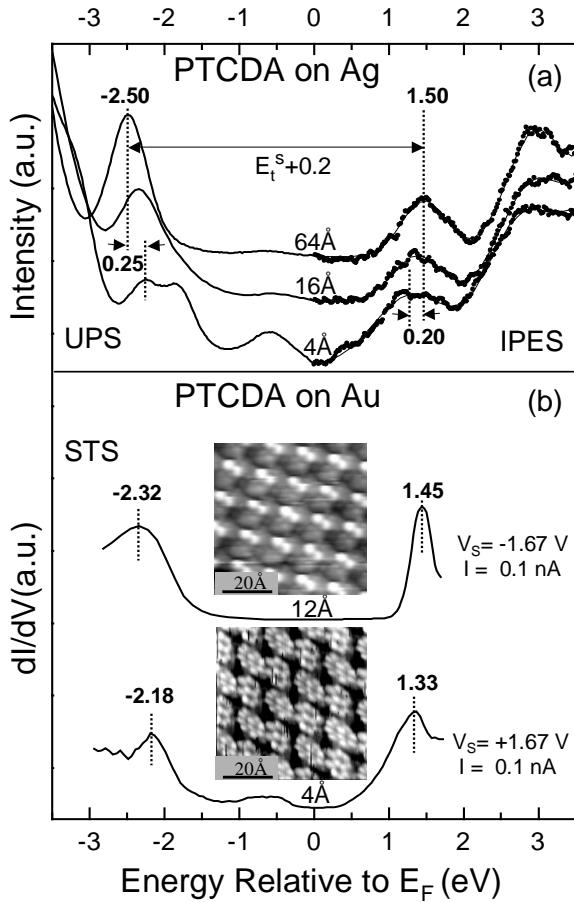


Fig. 2 (a) Composite UPS/IPES spectra as a function of PTCDA thickness on Ag. Energy scales are aligned by measuring the Fermi energy by UPS and IPES on Ag prior to PTCDA deposition. (b) $dI/dV(V)$ STS spectra of filled and empty states recorded for a monolayer (bottom) and a 2-3 molecular layer (top) film of PTCDA deposited on Au. The corresponding STM images of the films are shown. The curves were recorded at the same tunneling setpoints as the corresponding area scans.

Figure 2(a) shows UPS and IPES spectra of PTCDA (perylene-tetracarboxylic acid dianhydride) on silver. PTCDA is an excellent former of crystalline films whose structures are close, though not identical, to having a (102) plane of the bulk crystal in contact with the sub-

strate [4]. The measured transport gap on thick ($> 50\text{\AA}$) films is $E_t^S = 3.8$ eV on Ag, in excellent agreement with PTCDA on Au [3]. We use PTCDA on Ag rather than Au because the Au(5d) levels interfere with UPS of a monolayer. E_t^S includes a 0.2 eV intramolecular vibrational contribution [3] that reduces the UPS/IPES gap. This correction is the same for all PTCDA films. Careful analysis of peak positions indicates ~ 200 meV shifts of both the cation level (UPS) and anion level (IPES) between mono- and multilayer films.

Figure 2(b) shows the results of scanning tunneling spectroscopy (STS) on a monolayer (lower spectrum) and a 2-3 layer film (upper spectrum) of PTCDA on Au(111). These $dI/dV(V)$ spectra represent the density of filled and empty states involved in tunneling out of and into the layer, respectively. Each spectrum is the average of 25 spectra recorded at various points on highly ordered molecular layers. High-resolution scanning tunneling microscopy (STM) images of these layers, taken concomitantly with STS, show the characteristic difference [7] between monolayers, in which molecules are in contact with, and parallel to, the Au surface and appear symmetric, and second and subsequent layers, in which the tilt angle of molecules introduces an asymmetry in their STM image.

The tunneling spectrum of the monolayer shows peaks leading to $E_t^{ML} = 3.3$ eV for the energy difference between adding an electron or hole. Remarkably, this energy difference increases by about 0.25 eV on the 2-3 layer spectrum, in excellent agreement with the intermediate UPS/IPES spectra of a 16\AA film (Fig. 2a). Each peak shifts away from the Fermi level by a roughly equal amount with increasing coverage. We note that E_t^S and $E_t^S - E_t^{ML}$ show no dependence on dipoles at the metal-organic interface, which have opposite signs for PTCDA on Ag and Au [8]. The dipole at the PTCDA/Ag interface corresponds to electron transfer from the metal to interface molecules, which gives rise to the filled gap states at -0.6 and -1.8 eV on the 4\AA UPS spectrum. The broad feature around -0.6 eV on the 4\AA PTCDA/Au STS spectrum corresponds to the Au surface state, which is not eliminated by the deposition of organic molecules [9].

Reduced polarization energy at surfaces has long been appreciated on general grounds [1,2]. As anticipated and found for thin films of anthracene on Au, P_+ is about 200 meV smaller in the surface layer [10,11]. With similar reductions expected for P_- , the transport gap at the surface is *increased* some 400 meV from its bulk value, E_t . The gap increases near surfaces because vacuum is not polarizable. Conversely, E_t decreases near organic-metal interfaces due to the high polarizability of metals. These opposite contributions partially cancel in very thin films on metal substrates.

II. CHARGE REDISTRIBUTION

We note that E_t , which has been the focus of theoretical study [12,1] and governs bulk transport, is beyond the reach of the surface experimental techniques that access the outermost layers of the material and thus reflect E_t^S . Similarly, the transport gap E_t^M of the layer next to the metal is relevant for charge injection (Fig. 1(a)). A gap reduction of several hundred meV is significant since it directly alters interface barriers.

No theoretical treatment exists for the electronic polarization near surfaces and interfaces, which require an accuracy of ~ 100 meV. Methods to estimate P_{\pm} in the bulk have been developed, primarily for the acenes, based on the microelectrostatics of polarizable points that represent organic molecules [12,13]. Dielectric response of a neutral surface has also been studied [14]. We have recently developed an approach based on the analysis of charge redistribution in organic molecules [15], and demonstrated accurate calculations of P_+ , P_- , and energies of ion pairs in bulk PTCDA and anthracene crystals [16]. We apply here the same approach to calculate polarization in thin organic films.

In the zero-overlap limit, molecules comprising the crystal are quantum-mechanical objects interacting by classical forces. A self-consistent problem can be formulated [16] that treats molecules rigorously in the external fields of all other molecules. We describe charge redistribution in organic molecules in terms of the atom-atom polarizability tensor Π_{ij} that relates a change in the partial charge at an atom i due to the electrostatic potential $\phi_j = \phi(\mathbf{r}_j)$ at atom j :

$$\rho_i = \rho_i^{(0)} - \sum_j \Pi_{ij} \phi_j \quad (1)$$

$\rho_i^{(0)}$ are the atomic charges in an isolated molecule. The tensor Π_{ij} is a natural extension of the similar quantity in π -electron theory [17]. We compute Π_{ij} using INDO/S [18], which is a semiempirical Hamiltonian designed for spectroscopic molecular properties. Π_{ij} describes the major, ‘‘charge-induced’’ part of molecular polarizability α^C , which is augmented to reflect the actual polarizability α by introducing induced atomic dipoles $\boldsymbol{\mu}_i$ and distributing the difference $\tilde{\alpha} = \alpha - \alpha^C$ over 38 atoms of PTCDA in the spirit of submolecular methods [12]. Self-consistent equations for ρ_i and $\boldsymbol{\mu}_i$ are then solved for increasing cluster sizes of mesoscopic dimensions ($\sim 100\text{\AA}$), and the macroscopic limits are found. For neutral lattices the approach has yielded accurate anisotropic dielectric tensors of two representative organic crystals [15].

We use identical molecular inputs here to model PTCDA films as infinite slabs terminated by (102) planes next to a vacuum and a metal, respectively, as sketched in Fig. 1. The metal is taken as a constant-potential

plane at $z = 0$, a distance h from the innermost molecular layer. Image charges and dipoles at $z < 0$ ensure that the potential $\phi(z = 0) = 0$. Any $\phi(0) = C$ leads to the same result for $P = P_+ + P_-$, since one charge is stabilized and the other is destabilized. The metal-organic separation h is a model parameter that is related to Van der Waals radii.

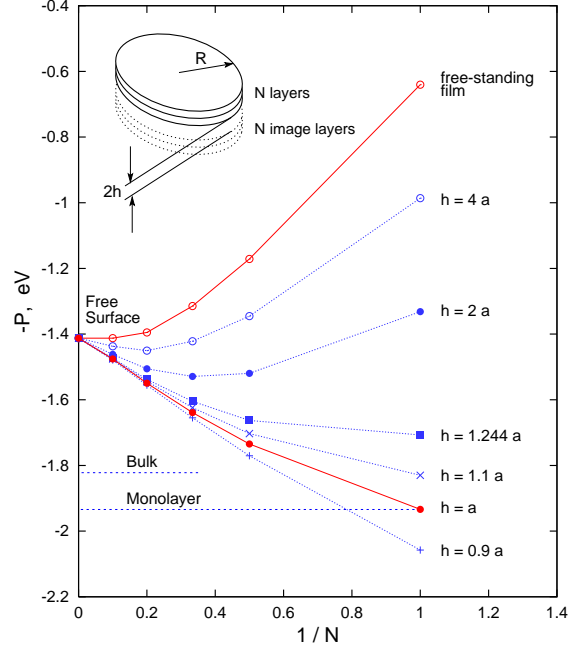


Fig. 3 Electronic polarization $P = P_+ + P_-$ at the outer layer of an N -layer film (Fig. 1) at separation h from the metal. The P values at the free surface ($N \rightarrow \infty$), a monolayer ($N = 1$), free-standing films ($h \rightarrow \infty$), and the bulk are indicated. A pill-box geometry with $R \sim 100\text{\AA}$ is used. The inset shows the transport gap, $E_t^{(n)}$, across a 10-layer film with $n = 1$ next to the metal and $n = 10$ at the outer surface.

We use a pill-box geometry, defined by the radius R (sketched in Fig. 3) with the ion placed in one of the layers near the center of the box. We initially find self-consistent atomic charges and induced dipoles $\bar{\rho}_i^k$ and $\bar{\boldsymbol{\mu}}_i^k$, $k = 1, \dots, N$ in a neutral film of N layers, where translational symmetry gives rapid convergence. We then consider pill-boxes of increasing diameter $2R$ to find self-consistent $\rho_i^a - \bar{\rho}_i^k$ and $\boldsymbol{\mu}_i^a - \bar{\boldsymbol{\mu}}_i^k$ for every molecule a in the pill-box. The largest systems ($2R = 135\text{\AA}$, $N = 10$) contain ~ 2400 PTCDA molecules and their images, and larger values of R can be used. P_+ is the energy difference between a neutral film and one containing a cation. P_- is the corresponding energy for an anion in the same position. We note that the energy of an infinite film is extensive, but the difference is finite and can be evaluated [16]. All data reported below is in the limit $R \rightarrow \infty$. P thus depends on which layer contains the ion.

III. RESULTS

For the ion in the outermost molecular layer in the limit $N \rightarrow \infty$ we obtain the free (102) surface polarization $P^S = 1.41$ eV. This limit does not depend on h or the metal. P^S is 0.41 eV less than the bulk value $P = 1.82$ eV [16]. The difference is consistent with experimental estimates [10] and corresponds to the surface correction $c = 1 - P^S/P = 0.23$, where the value inferred [3] from UPS and IPES spectra was $c \sim 0.25$.

Figure 3 gives results for PTCDA layers of finite thickness. Unlike bulk or free-surface calculations, which are essentially parameter-free, the finite layer data depends on h , which is the only way the metal enters our idealized model. The reasonable value $h = a$ places the metal plane one lattice spacing $a = 3.214$ Å from the innermost layer, which is also consistent with Van der Waals radii, and 10 % variations of h are shown in Fig. 3. We also computed P at $h = 1.244a$, $2a$ and $4a$, and extrapolated as $1/h$. The limit $h \rightarrow \infty$ gives the polarization at the surface of a free-standing film of N layers.

All curves in Fig. 3 converge to the free-surface value $P^S = 1.41$ eV. Using the curve $h = a$ we find the single monolayer value $P^{\text{ML}} = 1.93$ eV, which corresponds to the tunneling spectroscopy setup (Fig. 1(b)). We see that for a monolayer on the metal surface, the polarization energy is indeed close to the bulk value in line with the expected cancellation discussed above. The difference $P^{\text{ML}} - P^S = 0.52$ eV agrees with the experimental $E_t^S - E_t^{\text{ML}} = 0.45\text{--}0.50$ eV for PTCDA on Ag or Au. In fact, the agreement is slightly better since UPS/IPES data is for the films of finite thickness $N \sim 20$. The free-standing monolayer has $P = 0.64$ eV, which is about $E_t/3$. Such a big polarization is consistent with large in-plane polarizability of PTCDA molecules. These results for P are summarized for comparison in Table I.

Table I. $P_+ + P_-$ at various positions in the film

Bulk	1.82 eV
Free surface	1.41 eV
Monolayer, free-standing	0.64 eV
Monolayer on metal ($h = a$)	1.93 eV
Surface of a bilayer on metal ($h = a$)	1.73 eV
Layer next to metal, thick film ($h = a$)	2.21 eV

Analysis of UPS data for films of the electron-transport molecule Alq₃ [tris(8-hydroxy-quinoline)-aluminum] on silver [19] yields strikingly similar conclusions: the transport gap for a monolayer on metal substrate, E_t^{ML} , is equal to the inferred bulk value, and is about 400 meV narrower than the gap in the outermost surface layer of a thick film, E_t^S . Also, the inferred gap in the innermost layer of a thick film on metal surface, E_t^{M} , is about 400 meV less [19] than E_t^{ML} .

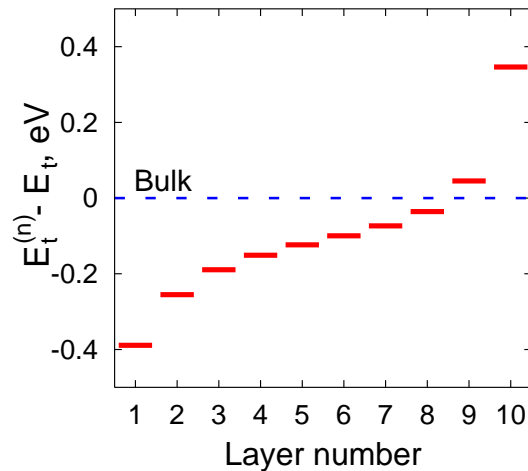


Fig. 4 Variation of the transport gap from the bulk value, $E_t^{(n)} - E_t$, across a 10-layer film with $n = 1$ next to the metal and $n = 10$ at the outer surface.

Figure 4 shows the variation of the transport gap E_t across a 10-layer PTCDA film on a metal substrate ($h = a$). We note that surface effects extend several layers into the sample. The long-range nature of surface polarization has been largely neglected. An influential early UPS study of 20Å vapor-deposited anthracene films on Au ascribed the 200 meV shift of P_+ to the single outermost layer [10]. The additivity of polarization contributions suggested [19] for Alq₃ is tacitly based on short-range interactions. Greater polarizability next to the metal is consistent with strong charge confinement to interfaces, as inferred recently for pentacene field-effect transistors with remarkable electronic characteristics [5]. In general, the 400 meV increase of $P_+ + P_-$ at the metal-organic interface is not shared equally by the electron and hole. The stabilization of either carrier by roughly 200 meV is important for matching transport levels in injection.

Weak overlap in molecular solids constitutes, in fact, a significant simplification over covalent bonding in inorganic semiconductors. Even though charge transport is critical for electronic applications, the picture of localized carriers is the proper zeroth-order approximation, to which the overlap (i.e. kinetic energy) should be considered as a perturbation. This does not by itself rule out the band-like description. Rather, charged quasiparticles are to be understood as surrounded by polarization clouds, likely affecting the bandwidths.

Our results for P_+ and P_- are exclusively electronic. Lattice relaxation around charges are considered to be small corrections ($\sim 10\%$) on general grounds [1,2]. The idealized model of image charges does not depend on the metal's Fermi energy or on surface dipoles, whose shifts cancel in $P = P_+ + P_-$. It also ignores surface states or surface reactions that are known to occur at specific organic/metal interfaces [6]. Since the self-consistent cal-

cultation requires the film's structure, it is not directly applicable to amorphous or structurally uncharacterized films.

Support of this work by the NSF (DMR-0097133) is gratefully acknowledged.

-
- [1] E.A. Silinsh and V. Capek, *Organic Molecular Crystals: Interaction, Localization and Transport Phenomena* (Am. Inst. Phys., New York, 1994).
- [2] M. Pope and C.E. Swenberg, *Electronic Processes in Organic Crystals* (Clarendon, Oxford, 1982).
- [3] I.G. Hill, A. Kahn, Z.G. Soos and R.A. Pascal, Jr., Chem. Phys. Lett. **327**, 181 (2000).
- [4] S.R. Forrest, Chem. Rev. **97**, 1793 (1997) and references therein.
- [5] J.H. Schön, S. Berg, Ch. Kloc, and B. Batlogg, Science **287**, 1022 (2000);
- [6] *Conjugated Polymer and Molecular Interfaces*, W.R. Salaneck, K. Seki, A. Kahn, and J.-J. Pireaux editors (Marcel Dekker, Inc., 2001).
- [7] I. Chizhov, A. Kahn, and G. Scoles, J. Crystal Growth **208**, 449 (2000).
- [8] I.G. Hill, A. Rajagopal, A. Kahn, and Y. Hu, Appl. Phys. Lett. **73**, 662 (1998).
- [9] J. Pflaum, G. Bracco, F. Schreiber, R. Colorado, Jr., O.E. Shmakova, T.R. Lee, G. Scoles, and A. Kahn, Surf. Sci. **498**, 89 (2002).
- [10] W.R. Salaneck, Phys. Rev. Lett. **40**, 60 (1978).
- [11] C.B. Duke, T.J. Fabish, and A. Paton, Chem. Phys. Lett. **49**, 133 (1977).
- [12] J.W. Rohleder and R.W. Munn, *Magnetism and Optics of Molecular Crystals* (Wiley, New York, 1992) and references therein.
- [13] G. Mazur and P. Petelenz, Chem. Phys. Lett. **324**, 161 (2000).
- [14] M. Malagoli and R.W. Munn, J. Chem. Phys. **112**, 6749 (2000)
- [15] Z.G. Soos, E.V. Tsiper, and R.A. Pascal Jr., Chem. Phys. Lett. **342**, 652 (2001).
- [16] E.V. Tsiper and Z.G. Soos, Phys. Rev. **B64**, 195124 (2001).
- [17] C.A. Coulson and H.C. Longuet-Higgins, Proc. Roy. Soc. (London) **A191**, 39 (1947).
- [18] M.C. Zerner, G.H. Loew, R.F. Kirchner, and U.T. Mueller-Westerhoff, J. Am. Chem. Soc., **102**, 589 (1980).
- [19] I.G. Hill, A.J. Mäkinen, and Z.H. Kafafi, J. Appl. Phys. **88**, 889 (2000).